Observer design for state and parameter estimation in a landslide model

Mohit Mishra, Gildas Besancon, Guillaume Chambon, Laurent Baillet

Observer design for state and parameter estimation in a landslide model

Mohit Mishra [*], **Gildas Besançon** [*], **Guillaume Chambon** [**], **Laurent Baillet** [***]

[*] *Univ. Grenoble Alpes, CNRS, Grenoble INP - Institute of Engineering, GIPSA-lab, 38000 Grenoble, France (e-mail: [mohit.mishra, gildas.besancon]@gipsa-lab.grenoble-inp.fr)*
[**] *Univ. Grenoble Alpes, INRAE, UR ETGR, Grenoble, France (e-mail: guillaume.chambon@inrae.fr)*
[***] *Univ. Grenoble Alpes, CNRS, ISTerre, Grenoble, France (e-mail: laurent.baillet@univ-grenoble-alpes.fr)*

Abstract: This paper presents an observer-based state and parameter estimation for the extended sliding-consolidation model of a landslide. This system is described by a pair of coupled Ordinary Differential Equation (ODE) and Partial Differential Equation (PDE), with a mixed boundary condition for the PDE. The coupling appears both in the ODE and in the Neuman boundary condition of the PDE. The observer consists of a copy of the PDE part of the system and Kalman-like observer for the ODE. It is shown to ensure exponential convergence of the state and parameter estimates by means of Lyapunov tool. Finally, a simulation result of the extended sliding-consolidation model is presented to illustrate the effectiveness of the proposed observer.

Keywords: State estimation, parameter estimation, extended sliding-consolidation model, coupled ODE-PDE system, observer.

1. INTRODUCTION

A landslide or slope destabilization is a gravity-driven downslope movement of rock, debris, or soil near earth's surface caused by heavy precipitation, flood, earthquakes, substantial snowmelt, or human activities such as construction work. Over the last decade, climate change (Gariano and Guzzetti, 2016) and rapid urbanization (Nyambod, 2010) have increased the frequency of occurrence of landslides. This, in turn, grabbed the attention towards the implementation of early warning systems (EWS) to take timely actions to reduce human and economic losses in advance of hazardous events (Krøgli et al., 2018). One of the significant components of EWS is environmental monitoring and forecasting (UN/ISDR, 2006). Environmental monitoring and forecasting are tools to assess the current status of an environment and establish the trends in environmental parameters. Information or data collected with the help of environmental monitoring are processed and often used in the assessment of risks related to the environment, e.g., weather forecast provides better predictions for tropical storms, hurricanes, and severe weather. In the past few years, developments in satellite remote sensing of the surface and atmosphere of the earth, numerical modeling, and data assimilation have improved the accuracy of weather forecasting.
Similarly, for anticipation/estimation of the hazards associated with landslide, a physics-based dynamical model, landslide monitoring, and heterogeneous data handling play a vital role. These physics-based dynamical models, e.g., sliding-consolidation model (Hutchinson, 1986), viscoplastic sliding-consolidation model (Corominas et al., 2005; Herrera et al., 2013; Bernardie et al., 2014) and extended sliding-consolidation model (Iverson, 2005) are sensitive to the initial conditions and parameters of the system. These sensitivities can be taken into account by simulating a model and iteratively adjusting the initial conditions and parameter values to obtain consistency with measured data, i.e., by adjoint method (Nguyen et al., 2016). Another efficient approach is to run a model over a time and continually fine-tune it to synchronize with incoming data, i.e., Kalman filter like approach. Therefore, a comprehensive evaluation of landslide hazards involves multi-dimensional problems, which require a multi-disciplinary approach viz. geophysics, mechanics, signal/data processing, dynamical systems, control theory, and information technologies.

In this context, the present paper proposes an observer design for state and parameter estimation in an extended sliding-consolidation of a landslide with full convergence analysis. The key feature of this model is mechanical feedback, which might be responsible for the diverse rates of landslide motion (from steady creeping motion to runaway acceleration). This model is made of an Ordinary Differential Equation (ODE) coupled with a Partial Differential Equation (PDE) subject to mixed boundary conditions, with the PDE state entering into the ODE dynamics, and the ODE state affecting the Neuman boundary of the PDE. The observer design relies on a measurement

⋆ This work is supported by the French National Research Agency in the framework of the Investissements dAvenir program (ANR-15-IDEX-02)

on the ODE. Notice that observer is known to be an efficient tool for state estimation, or joint state and parameter estimation (starting with the famous Extended Kalman Filter). In recent years, it has also been extended to systems with distributed dynamics, with examples in open channel level control (Besançon et al., 2008) or monitoring (Bedjaoui et al., 2009), backstepping boundary observer for a class of linear first-order hyperbolic systems with spatially-varying parameters (Di Meglio et al., 2013), robust state estimation based on a boundary output injection for a class of convection-diffusion-reaction systems (Besançon et al., 2013), matrix inequality-based observer for transport-reaction systems (Schaum et al., 2014), backstepping adaptive observer-based state and parameter estimation for hyperbolic systems with uncertain boundary parameters and its application to underbalanced drilling (Di Meglio et al., 2014), adaptive observer for coupled linear hyperbolic PDEs with unknown boundary parameters based on swapping (Anfinsen et al., 2016), and even with extension to coupled ODE-PDE like in the case of high-gain type observer for a class of nonlinear ODE-PDE cascade systems (Ahmed-Ali et al., 2015), and boundary observer based on the Volterra integral transformation for hyperbolic PDE-ODE cascade systems (Hasan et al., 2016). In the present paper, the coupled PDE-ODE observer problem under consideration is addressed by basically combining a copy of PDE dynamics with a Kalman-like observer for the ODE.

The structure of the paper is as follows: A landslide model depicting landslide behavior and the problem statement is given in Section 2. Section 3 presents the proposed observer with full convergence analysis. In Section 4, the simulation results demonstrate the effectiveness of the proposed observer. Finally, some conclusions and future directions of the work are discussed in Section 5.

2. PROBLEM FORMULATION

Extended sliding-consolidation model

The extended sliding-consolidation model (Iverson, 2005) is based on a representation of the landslide as a rigid block overlying a thin shear zone, where landslide (slide block) motion is opposed by basal Coulomb friction and regulated by basal pore fluid pressure. For the analysis purpose, the model assumes two components of basal pore pressure: i) imposed pore pressure p_i due rain infiltration and ii) development of excess pore pressure p_e in response to dilation or contraction of the basal shear zone. The motion of the slide block and excess pore pressure evolution are described by Eq.(1) and (2) respectively.

Momentum equation

$$\begin{aligned}\frac{d^2u_x}{dt^2} = \frac{dv_x}{dt} &= gcos\psi\,[sin(\theta-\psi) - cos(\theta-\psi)tan\phi] \\ &+ \frac{cos^2\psi tan\phi}{\rho Z}\,\{p_i(0,t) + p_e(0,t)\}\end{aligned} \tag{1}$$

Excess pore pressure diffusion equation

$$\begin{aligned}\frac{\partial p_e(z,t)}{\partial t} &= D\frac{\partial^2 p_e(z,t)}{\partial z^2} \\ \frac{\partial p_e(0,t)}{\partial z} &= \frac{\rho_w g\psi}{K}v_x, \\ p_e(Z,t) &= 0\end{aligned} \tag{2}$$

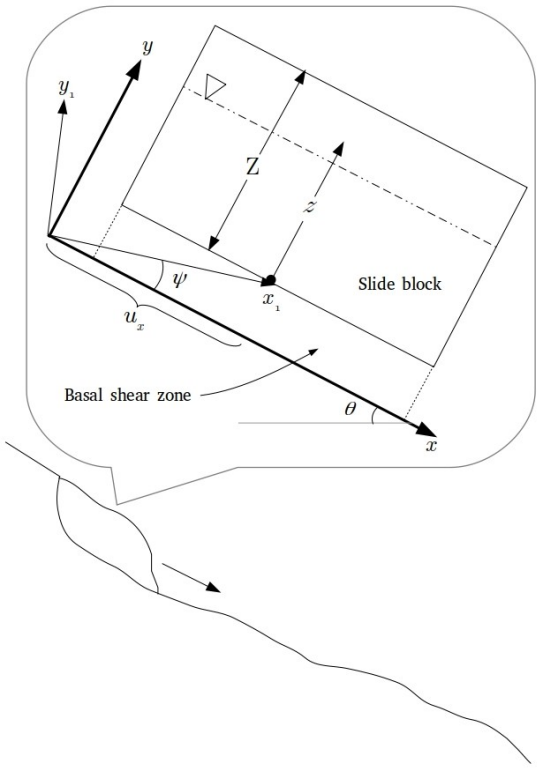

Fig. 1. The coordinate systems, geometric variables and material property of the slide block

where ϕ: friction angle (mechanical strength),
ψ: dilatancy angle of the material,
ρ: soil density,
ρ_w: pore water density,
D: diffusion coefficient,
K: hydraulic conductivity,
g: acceleration due to gravity,
θ: sliding angle,
$u_x(t)$ and $v_x(t)$: displacement and velocity of the slide block respectively (along x-axis),
$p_i(0,t)$: imposed pore pressure at the slide block base,
$p_e(z,t)$: excess pore pressure distribution,
$\partial p_e(0,t)/\partial z = \rho_w g\psi v_x/K$: Neuman boundary condition, and $p_e(Z,t) = 0$: Dirichlet boundary condition of the excess pore pressure diffusion equation.

$z \in [0, Z]$ with Z the spatial domain length (slide block thickness), and $t \geqslant 0$ is the time. In addition, v_{x_0} and p_{e_0} are initial values of v_x and p_e respectively. Coordinate z translates with the base of the slide block such that with dilation or contraction of shear zone the base of the slide block is always located at $z = 0$ as shown in Fig. 1.

In this model, rate of landslide motion depends on the dilatancy angle (ψ), which is generally difficult to measure. Also, this model is sensitive to the friction angle (ϕ) of the soil. Assuming that the other parameters can be obtained from some knowledge on soil characteristics and landslide geometry, this paper is thus concerned with the estimation of ϕ and ψ, along with the system state variables v_x and $p_e(x,t)$. This will be done assuming further some known imposed pore pressure time series, as well as some measured velocity time series.

3. OBSERVER-BASED STATE AND PARAMETER ESTIMATION

3.1 Normalized and transformed system equations

In order to address the observer problem, let us first normalize the system equations by introducing dimensionless variables defined as

$$\begin{aligned} z^* = \frac{z}{Z}, \quad t^* = \frac{t}{Z^2/D}, \quad v_x^* = \frac{v_x}{g(Z^2/D)}, \\ p_i^* = \frac{p_i}{\rho_w g Z} \quad \& \quad p_e^* = \frac{p_e}{\rho_w g Z}. \end{aligned} \tag{3}$$

Then, consider a transformation

$$\bar{p}_e^*(z^*, t^*) = \left[\frac{K/g}{\psi(Z^2/D)}\right] p_e^*(z^*, t^*) \tag{4}$$

and set

$$\begin{aligned} f_0 &= cos\psi\left[sin(\theta-\psi) - cos(\theta-\psi)tan\phi\right], \\ f_1 &= \frac{\rho_w}{\rho} cos^2\psi tan\phi \quad \& \quad f_2 = \left(\frac{Z^2/D}{K/g}\right)\psi f_1 \end{aligned} \tag{5}$$

where f_0, f_1 and f_2 are augmentative states depending on the parameter values i.e. $\dot{f}_0 = \dot{f}_1 = \dot{f}_2 = 0$. Now, substituting (3), (4), and (5) in (1) and (2) gives following system equations (Note that from now on notation ' $\cdot$ ' denotes d/dt^*):

$$\begin{bmatrix} \dot{v}_x^* \\ \dot{f}_0 \\ \dot{f}_1 \\ \dot{f}_2 \end{bmatrix} = \overbrace{\begin{bmatrix} 0 & 1 & p_i^*(0,t^*) & \bar{p}_e^*(0,t^*) \\ 0 & 0 & 0 & 0 \\ 0 & 0 & 0 & 0 \\ 0 & 0 & 0 & 0 \end{bmatrix}}^{\mathrm{A}(t^*)} \begin{bmatrix} v_x^* \\ f_0 \\ f_1 \\ f_2 \end{bmatrix} \tag{6}$$

$$\begin{aligned} y &= C\begin{bmatrix} v_x^* & f_0 & f_1 & f_2 \end{bmatrix}^\top \\ \frac{\partial \bar{p}_e^*(z^*,t^*)}{\partial t^*} &= \frac{\partial^2 \bar{p}_e^*(z^*,t^*)}{\partial z^{*2}} \\ \frac{\partial \bar{p}_e^*(0,t^*)}{\partial z^*} &= v_x^* \\ \bar{p}_e^*(1,t^*) &= 0 \end{aligned} \tag{7}$$

where $C = [1\ 0\ 0\ 0]$. This new form will be used for observer design. Here system transformation simplifies system equations while normalization helps to define space domain as $0 \le z^* \le 1$, which will facilitate the convergence proof of observer.

3.2 Observer Design

For the sake of clarity, let us recall some notations, Poincaré's inequality, Agmon's inequality and definition of regular persistence which will be used later in the convergence proof of the proposed scheme.

Notations: For a given $x \in \mathbb{R}^n$, $\|x\|$ and $\|x\|_{H_1}$ denotes its usual Euclidean norm and H_1 norm respectively.

Poincaré's inequality. (Besançon et al., 2013) Let $g = g(x)$ be continously differentiable function on $[0,1]$ with $g(0) = 0$ or $g(1) = 0$, then

$$\int_0^1 g^2(x)dx \le \frac{1}{\pi^2}\int_0^1 g_x^2(x)dx < \int_0^1 g_x^2(x)dx$$

where g_x is the first order derivative of g w.r.t. x.

Agmon's inequality. (Krstic and Smyshlyaev, 2008) For a function $g(x) \in H_1$ on $[0,1]$ following inequality holds

$$\max_{x\in[0,1]} |g(x)|^2 \le 2\sqrt{\int_0^1 g(x)^2 dx}\sqrt{\int_0^1 g_x(x)^2 dx}.$$

Regular persistence. (Besançon et al., 1996) For regularly persistent $p_i^*(0,t^*)$ and initial conditions in system (6)-(7), $\exists\ T > 0$, $\alpha > 0$, $t_0^* > 0$ such that

$$\int_{t^*}^{t^*+T} \phi^\top(\tau, t^*) C^\top C \phi(\tau, t^*) d\tau \ge \alpha I \quad \forall t^* \ge t_0^* \tag{8}$$

where $\phi(\tau, t^*)$ is the state transition matrix of (6).

The main result can be stated as follows:

Theorem 1. For system (6)-(7) with available measurement $y = v_x^*$, regularly persistent known imposed pore pressure time series $p_i^*(0,t^*)$ and any initial condition, *observer* (9)-(10) guarantees that $\hat{\bar{p}}_e^*(z^*,t^*) - \bar{p}_e^*(z^*,t^*)$, $\hat{v}_x^*(t^*) - v_x^*(t^*)$, $\hat{f}_0(t^*) - f_0$, $\hat{f}_1(t^*) - f_1$, and $\hat{f}_2(t^*) - f_2$ converge to 0 as $t^* \to \infty$ for all $0 \le z^* \le 1$, and $\theta \ge \theta_0$ for some $\theta_0 > 0$.

$$\begin{aligned} \frac{\partial \hat{\bar{p}}_e^*(z^*,t^*)}{\partial t^*} &= \frac{\partial^2 \hat{\bar{p}}_e^*(z^*,t^*)}{\partial z^{*2}} \\ \frac{\partial \hat{\bar{p}}_e^*(0,t^*)}{\partial z^*} &= y, \\ \hat{\bar{p}}_e^*(1,t^*) &= 0 \end{aligned} \tag{9}$$

$$\begin{bmatrix} \dot{\hat{v}}_x^* \\ \dot{\hat{f}}_0 \\ \dot{\hat{f}}_1 \\ \dot{\hat{f}}_2 \end{bmatrix} = \overbrace{\begin{bmatrix} 0 & 1 & p_i^*(0,t^*) & \hat{\bar{p}}_e^*(0,t^*) \\ 0 & 0 & 0 & 0 \\ 0 & 0 & 0 & 0 \\ 0 & 0 & 0 & 0 \end{bmatrix}}^{\hat{A}(t^*)} \begin{bmatrix} \hat{v}_x^* \\ \hat{f}_0 \\ \hat{f}_1 \\ \hat{f}_2 \end{bmatrix} - \hat{S}^{-1}C^\top\left[\hat{v}_x^* - y\right] \tag{10}$$

$$\dot{\hat{S}}(t^*) = -\theta\hat{S}(t^*) - \hat{A}(t^*)^\top\hat{S}(t^*) - \hat{S}(t^*)\hat{A}(t^*) + C^\top C$$

Proof.
Define estimation errors: $e(z^*,t^*) := \hat{\bar{p}}_e^*(z^*,t^*) - \bar{p}_e^*(z^*,t^*)$ and

$$E(t^*) = \begin{bmatrix} \hat{v}_x^*(t^*) \\ \hat{f}_0(t^*) \\ \hat{f}_1(t^*) \\ \hat{f}_2(t^*) \end{bmatrix} - \begin{bmatrix} v_x^*(t^*) \\ f_0 \\ f_1 \\ f_2 \end{bmatrix}.$$

Then, they satisfy equations:

$$\begin{aligned} e_t(z^*,t^*) &= e_{zz}(z^*,t^*) \\ e_z(0,t^*) &= 0 \\ e(1,t^*) &= 0 \\ e(z^*,0) &= e_0(z^*) \end{aligned} \tag{11}$$

and

$$\dot{E} = \left[\hat{A}(t^*) - \hat{S}^{-1}(t^*)C^\top C\right]E + \begin{bmatrix} \left\{\hat{\bar{p}}_e^*(0,t^*) - \bar{p}_e^*(0,t^*)\right\} f_2 \\ 0 \\ 0 \\ 0 \end{bmatrix} \tag{12}$$

where e_z and e_{zz} are first and second order derivatives of e w.r.t. z^* respectively, and e_t is the first order derivative of e w.r.t. t^*. Let us study the convergence of both estimation errors by *Lyapunov function approach* separately.

• Convergence of $e(z^*,t^*)$:

A candidate Lyapunov function based on the classical energy function is considered as (Krstic and Smyshlyaev, 2008):

$$V_1(t^*) := \frac{1}{2}\int_0^1 e^2(z^*,t^*)dz^* + \frac{1}{2}\int_0^1 e_z^2(z^*,t^*)dz^*. \tag{13}$$

Differentiating (13) w.r.t. t^*, by using integration by parts and (11), we get:

$$\dot{V}_1(t^*) = -\int_0^1 e_z^2 dz^* - \int_0^1 e_{zz}^2 dz^* \leq -\int_0^1 e_z^2 dz^*$$
$$\dot{V}_1(t^*) \leq -\frac{1}{2}\int_0^1 e_z^2 dz^* - \frac{1}{2}\int_0^1 e_z^2 dz^*.$$

Finally, by using Poincaré's inequality and (13), we obtain $\dot{V}_1(t^*) \leq -V_1(t^*)$ which implies $V_1(t^*) \leq exp(-t^*)V_1(0)$ i.e.,

$$\begin{aligned}\int_0^1 [e^2(z^*,t^*) + e_z^2(z^*,t^*)]dz^* \\ \leq exp(-t^*)\left\{\int_0^1 \left[e^2(z^*,0) + e_z^2(z^*,0)\right] dz^*\right\} \\ \leq exp(-t^*)\left\|e(z^*,0))\right\|_{H_1}^2.\end{aligned} \tag{14}$$

Condition above proves that $\int_0^1 e(z^*,t^*)dz^* \to 0$ as $t^* \to \infty$ but this does not imply that $e(z^*,t^*)$ goes to 0 $\forall z^* \in (0,1)$. Therefore, by Agmon's inequality we obtain

$$\begin{aligned}\max_{z^*\in[0,1]} |e(z^*,t^*)|^2 &\leq 2\sqrt{\int_0^1 e^2(z^*,t^*)dz^*}\sqrt{\int_0^1 e_z^2(z^*,t^*)dz^*} \\ &\leq \int_0^1 e^2(z^*,t^*)dz^* + \int_0^1 e_z^2(z^*,t^*)dz^*.\end{aligned}$$

Now, by using (14) we get

$$\max_{z^*\in[0,1]} |e(z^*,t^*)|^2 \leq exp(-t^*)\left\|e(z^*,0))\right\|_{H_1}^2. \tag{15}$$

This conclude that $e(z^*,t^*)$ converges to 0 as $t^* \to \infty$ $\forall z^* \in [0,1]$.

• Convergence of $E(t^*)$:

Remember first regular persistence (8) and its consequence on the following Lyapunov differential equation:

$$\dot{S}(t^*) = -\theta S(t^*) - A^\top(t^*)S(t^*) - S(t^*)A(t^*) + C^\top C, \quad S(0) > 0.$$

From (Besançon et al., 1996) for instance, $\exists \theta_0 > 0$ such that $\forall \theta \geq \theta_0$, $\exists \alpha_1 > 0, \alpha_2 > 0, t_0^* > 0 : \forall t^* \geq t_0^*$

$$\alpha_1 I \leq S(t^*) \leq \alpha_2 I$$

Notice then that $\hat{A} = A + \Delta$ with $\|\Delta\|$ exponentially vanishing. It results from Lemma 3.1 in (Besançon et al., 1996) that solution of

$$\dot{\hat{S}}(t^*) = -\theta\hat{S}(t^*) - \hat{A}^\top(t^*)\hat{S}(t^*) - \hat{S}(t^*)\hat{A}(t^*) + C^\top C, \quad \hat{S}(0) > 0$$

satisfies $\left\|\hat{S}(t^*) - S(t^*)\right\| \leq \lambda e^{-\xi t^*}$ for $\lambda > 0$, $\xi > 0$ and θ large enough. From this, θ can be chosen so that $\hat{S}(t^*)$ also satisfies boundedness of the form

$$\hat{\alpha}_1 I \leq \hat{S}(t^*) \leq \hat{\alpha}_2 I, \quad \forall t^* \geq t_0^*, \hat{\alpha}_1, \hat{\alpha}_2 > 0. \tag{16}$$

Hence, we can consider a candidate Lyapunov function as:

$$V_2(t^*) := E(t^*)^\top \hat{S}(t^*)E(t^*). \tag{17}$$

Firstly, differentiating (17) w.r.t. time, using (10) and (12) we get

$$\begin{aligned}\dot{V}_2(t^*) &= 2E(t^*)^\top \hat{S}(t^*)\dot{E}(t^*) + E(t^*)^\top \dot{\hat{S}}(t^*)E(t^*) \\ &= -\theta E(t^*)^\top \hat{S}(t^*)E(t^*) + 2E(t^*)^\top \hat{S}(t^*)\begin{bmatrix} e(0,t^*)f_2 \\ 0 \\ 0 \\ 0 \end{bmatrix} \\ &\leq -\theta V_2 + 2\left\|E\right\|\left\|\hat{S}(t^*)\right\| |e(0,t^*)|\, f_2\end{aligned}$$

Then, from (15), (16) and (17) we obtain

$$\dot{V}_2(t^*) \leq -\theta V_2 + 2\sqrt{V_2(t^*)/\hat{\alpha}_2}\hat{\alpha}_2 exp(-t^*)\left\|e(0,0))\right\|_{H_1}^2 f_2$$

Now, dividing both sides of the equation by $2\sqrt{V_2(t^*)}$ we get

$$\frac{\mathrm{d}}{\mathrm{d}t^*}\sqrt{V_2(t^*)} \leq -\frac{\theta}{2\hat{\alpha}_2}\sqrt{V_2(t^*)} + \sqrt{\hat{\alpha}_2}exp(-t^*)\left\|e(0,0))\right\|_{H_1}^2 f_2.$$

Integrating both sides of the equation gives

$$\begin{aligned}\sqrt{V_2(t^*)} &\leq exp\left(-\frac{\theta}{2\hat{\alpha}_2}t^*\right)\sqrt{V_2(0)} \\ &+ \int_0^{t^*} exp\left(-\frac{\theta}{2\hat{\alpha}_2}(t^*-\tau)\right)\sqrt{\hat{\alpha}_2}exp(-\tau)\left\|e(0,0))\right\|_{H_1}^2 f_2 d\tau\end{aligned}$$

which implies that $\sqrt{V_2(t^*)}$ exponentially decays to zero and so $E(t^*) \to 0$ as $t^* \to \infty$.

4. SIMULATION RESULTS

4.1 Measured velocity time-series

To validate the effectiveness of the designed observer, a slide block velocity time-series is generated by solving the system equations (1)-(2), and then white Gaussian noise is added to it (Signal to noise ratio = 20 dB). The parameter values (Iverson, 2005) and initial values used for the simulation are indicated in Table 1 (Initial values are chosen differently than initial values for the observer to validate the performance). The momentum equation (1) is solved by a stepwise analytical method, and the numerical solution of the pore pressure diffusion equation (2) is obtained with the Crank-Nicolson method. In the simulations, imposed pore pressure time-series $p_i(0,t)$ representing rainfall variations is assumed as shown in Fig 2. The value of imposed pore pressure assumed to be greater than or equal to p_{crit} given as

$$p_{crit} = \frac{gcos\psi\,[cos(\theta-\psi)tan\phi - sin(\theta-\psi)]}{cos^2\psi tan\phi/\rho Z},$$

which corresponds to the value of pore pressure above which slide block starts to accelerate. Simulated excess pore pressure and velocity time series (with noise) are shown in Fig. 2 and Fig. 3 respectively. At each time step of solving (1)-(2) variables t, $p_i(0,t)$ and $v_x(t)$ are normalized using (3), so as to obtain t^*, $p_i^*(0,t^*)$ and $v_x^*(t^*)$ which act as input to observer.

Table 1. Parameter Values

Parameters	**Value**	**Unit**
Initial velocity, v_0	2.4×10^{-2}	mm/s
Initial excess pore pressure, p_{e_0}	-46.6	Pa
Simulation time, T	1000	s
Time step, Δt	0.01	s
Space step, Δz	0.0066	m
Diffusion coefficient, D	3×10^{-3}	m^2/s
Acceleration due to gravity, g	9.8	m/s^2
Slide block thickness, Z	0.65	m
Hydraulic conductivity, K	2×10^{-5}	m/s
Plane inclination angle, θ	31	deg
Slide block mass density, ρ	2000	kg/m^3
Pore water density, ρ_w	1000	kg/m^3
Friction angle, ϕ	**35**	deg
Dilatancy angle, ψ	**6**	deg

4.2 Observer results

In the simulation result, we are interested in the estimation of friction angle ϕ, dilatancy angle ψ, velocity of the slide

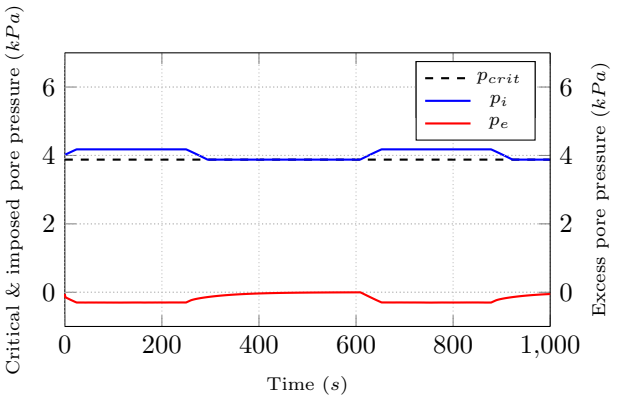

Fig. 2. Critical, imposed pore pressure and simulated excess pore pressure

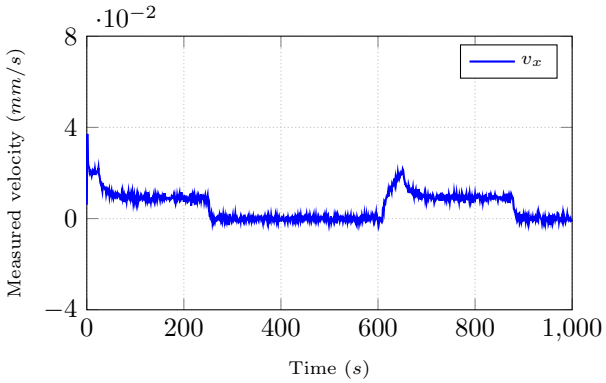

Fig. 3. Synthetic measured velocity time-series

block v_x, and basal excess pore pressure $p_e(0,t)$ assuming other parameter values and imposed pore pressure are known along with synthetic slide block velocity measurement. For initial states given in Table 2 (chosen such that initial guess for the ϕ and ψ are 55° and 3° respectively), observer (9)-(10) gives, estimates of the slide block velocity $\hat{v}_x^*$, excess pore pressure $\hat{p}_e^*(z,t)$, augmentative states $\hat{f}_0$, $\hat{f}_1$ and $\hat{f}_2$.

Table 2. Initial states for the observer

State	Value
Initial velocity, $\hat{v}_x^*(0)$	0
Initial excess pore pressure, $\hat{p}_e^*(z^*,0)$	0
Initial augmentative state, $\hat{f}_0(0)$	-0.7895
Initial augmentative state, $\hat{f}_1(0)$	0.7114
Initial augmentative state, $\hat{f}_2(0)$	2.5691×10^6

Notice that for observer (9)-(10) space step $\Delta z^* = \frac{\Delta z}{Z} = 0.01$ and time step $\Delta t^* = \frac{\Delta t}{Z^2/D} = 7.1 \times 10^{-5}$. Based on estimates from observer, at each time step firstly dilatancy angle $\hat{\psi}$ and mechanical strength $\hat{\phi}$ are reconstructed by using Eq. (18) and (19) respectively.

$$\hat{\psi}(t^*) = \frac{\hat{f}_2(t^*)}{\hat{f}_1(t^*)} \times \left(\frac{K/g}{Z^2/D}\right) \tag{18}$$

$$\hat{\phi}(t^*) = tan^{-1}\left[\frac{\rho \hat{f}_1(t^*)}{\rho_w cos^2 \hat{\psi}(t^*)}\right] \tag{19}$$

Then, basal excess pore pressure $\hat{p}_e^*(0,t^*)$ is obtained by inverse transformation

$$\hat{p}_e^*(0,t^*) = \left[\frac{Z^2/D}{K/g}\right] \hat{\psi}(t^*)\hat{\tilde{p}}_e^*(0,t^*). \tag{20}$$

Observer (9)-(10) is solved for simulation time $T^* = \frac{T}{Z^2/D} = 7.1$. After completion of the simulation, all desired estimates $\hat{\psi}(t)$, $\hat{\phi}(t)$, $\hat{v}_x(t)$, and $\hat{p}_e(0,t)$ are reconstructed from $\hat{\psi}(t^*)$, $\hat{\phi}(t^*)$, $\hat{v}_x^*(t^*)$, and $\hat{p}_e^*(0,t^*)$ using (3).

A convergence of the state and parameter estimates can be seen in Fig. 4, Fig. 5, Fig. 6 and Fig. 7. In this simulation, the estimated parameter values are $\psi = 5.97°$ and $\phi = 35.5°$ with the relative error between estimated and desired values 0.5% and 1.42% respectively.

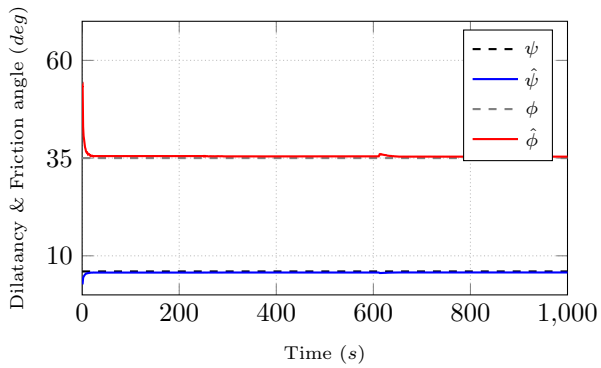

Fig. 4. Time evolution of the parameter estimate $\hat{\psi}$ & $\hat{\phi}$

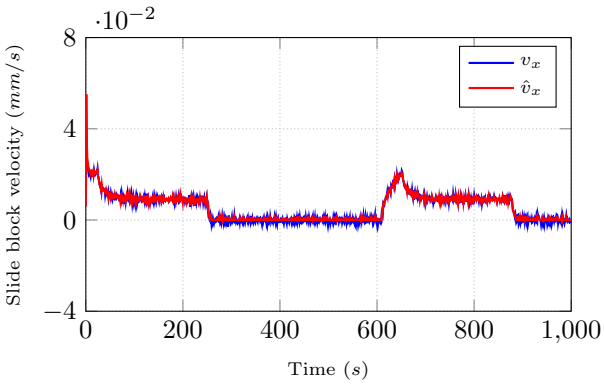

Fig. 5. Time evolution of the state estimate $\hat{v}_x$

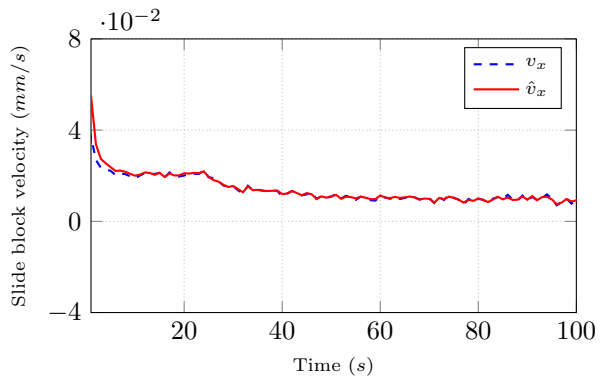

Fig. 6. Time evolution of the state estimate $\hat{v}_x$ (Zoomed-in)

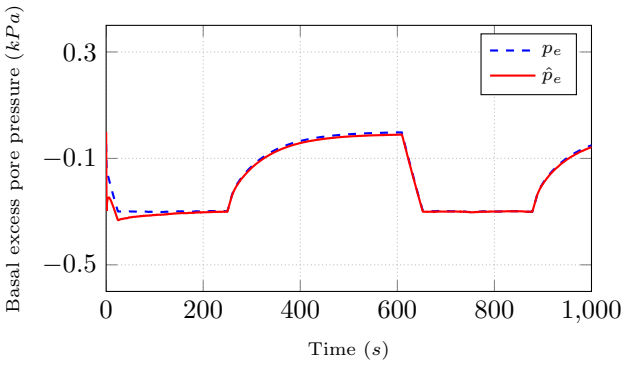

Fig. 7. Time evolution of the state estimate $\hat{p}_e(0,t)$

5. CONCLUSIONS AND FUTURE WORK

In this paper, we designed an observer for state and parameter estimation of a landslide. Firstly, we considered the extended sliding-consolidation model depicting a landslide behavior, which is a coupled ODE-PDE system. Secondly, the model is transformed and simplified to utilize the Kalman filter like approach for the observer design. Then the exponential stability of estimation errors has been validated with the help of candidate Lyapunov functional. Lastly, parameter values (friction and dilatancy angle) and states of the system have been well estimated.

Based on this result, a future direction for work will be to validate the effectiveness of the designed observer on actual field measurements.

REFERENCES

Ahmed-Ali, T., Giri, F., Krstic, M., and Lamnabhi-Lagarrigue, F. (2015). Observer design for a class of nonlinear ODE-PDE cascade systems. *Systems & Control Letters*, 83, 19–27. doi: https://doi.org/10.1016/j.sysconle.2015.06.003.

Anfinsen, H., Diagne, M., Aamo, O.M., and Krstic, M. (2016). An Adaptive Observer Design for $n+1$ Coupled Linear Hyperbolic PDEs Based on Swapping. *IEEE Transactions on Automatic Control*, 61(12), 3979–3990. doi:10.1109/TAC.2016.2530624.

Bedjaoui, N., Weyer, E., and Bastin, G. (2009). Methods for the localization of a leak in open water channels. *Networks & Heterogeneous Media*, 4(1556-1801-2009-2-189), 189–210. doi:10.3934/nhm.2009.4.189.

Bernardie, S., Desramaut, N., Malet, J., Maxime, G., and Grandjean, G. (2014). Prediction of changes in landslide rates induced by rainfall. *Landslides*, 12. doi: 10.1007/s10346-014-0495-8.

Besançon, G., Bornard, G., and Hammouri, H. (1996). Observer Synthesis for a Class of Nonlinear Control Systems. *European Journal of Control*, 2(3), 176–192. doi:10.1016/S0947-3580(96)70043-2.

Besançon, G., Dulhoste, J.F., and Georges, D. (2008). Nonlinear Observer-Based Feedback for Open-Channel Level Control. *Journal of Hydraulic Engineering*, 134. doi:10.1061/(ASCE)0733-9429(2008)134:9(1267).

Besançon, G., Pham, T.V., and Georges, D. (2013). Robust state estimation for a class of convection-diffusion-reaction systems. *IFAC Proceedings Volumes*, 46(26), 203–208. doi:10.3182/20130925-3-FR-4043.00012. 1st IFAC Workshop on Control of Systems Governed by Partial Differential Equations.

Corominas, J., Moya, J., Ledesma, A., Lloret, A., and Gili, J. (2005). Prediction of ground displacements and velocities from groundwater level changes at the Vallcebre landslide (Eastern Pyrenees, Spain). *Landslides*, 2, 83–96. doi:10.1007/s10346-005-0049-1.

Di Meglio, F., Bresch-Pietri, D., and Aarsnes, U.J.F. (2014). An adaptive observer for hyperbolic systems with application to UnderBalanced Drilling. *IFAC Proceedings Volumes*, 47(3), 11391–11397. doi: 10.3182/20140824-6-ZA-1003.02365. 19th IFAC World Congress.

Di Meglio, F., Krstic, M., and Vazquez, R. (2013). A backstepping boundary observer for a class of linear first-order hyperbolic systems. In *2013 European Control Conference (ECC)*, 1597–1602. doi: 10.23919/ECC.2013.6669563.

Gariano, S.L. and Guzzetti, F. (2016). Landslides in a changing climate. *Earth-Science Reviews*, 162, 227–252. doi:10.1016/j.earscirev.2016.08.011.

Hasan, A., Aamo, O.M., and Krstic, M. (2016). Boundary observer design for hyperbolic PDE-ODE cascade systems. *Automatica*, 68, 75–86. doi: 10.1016/j.automatica.2016.01.058.

Herrera, G., Fernandez-Merodo, J.A., Mulas, J., Pastor, M., Luzi, G., and Monserrat, O. (2013). A landslide forecasting model using ground based SAR data: The Portalet case study. *Engineering Geology*, 105, 220–230. doi:10.1016/j.enggeo.2009.02.009.

Hutchinson, J.N. (1986). A sliding-consolidation model for flow slides. *Canadian Geotechnical Journal*, 23(2), 115–126. doi:10.1139/t86-021.

Iverson, R. (2005). Regulation of landslide motion by dilatancy and pore pressure feedback. *J. Geophys. Res*, 110. doi:10.1029/2004JF000268.

Krøgli, I.K., Devoli, G., Colleuille, H., Boje, S., Sund, M., and Engen, I.K. (2018). The Norwegian forecasting and warning service for rainfall- and snowmelt-induced landslides. *Nat. Hazards Earth Syst. Sci.*, 18(5), 1427–1450. doi:10.5194/nhess-18-1427-2018.

Krstic, M. and Smyshlyaev, A. (2008). *Boundary Control of PDEs: A Course on Backstepping Designs*. Society for Industrial and Applied Mathematics, USA.

Nguyen, V.T., Georges, D., and Besançon, G. (2016). State and parameter estimation in 1-D hyperbolic PDEs based on an adjoint method. *Automatica*, 67, 185–191. doi: 10.1016/j.automatica.2016.01.031.

Nyambod, E.M. (2010). Environmental Consequences of Rapid Urbanisation: Bamenda City, Cameroon. *Journal of Environmental Protection*, 1, 15–23. doi: 10.4236/jep.2010.11003.

Schaum, A., Moreno, J.A., Fridman, E., and Alvarez, J. (2014). Matrix inequality-based observer design for a class of distributed transport-reaction systems. *International Journal of Robust and Nonlinear Control*, 24(16), 2213–2230. doi:10.1002/rnc.2981.

UN/ISDR (2006). Developing Early Warning Systems: A checklist. *EWC III Third International Conference on Early Warning, From concept to action*. URL `https://www.unisdr.org/unisdr-archives/2006/ppew/info-resources/ewc3/checklist/English.pdf`.